RANS Simulations of Free Maneuvers with Moving Rudders and Propellers Using Overset Grids in OpenFOAM

Conference Paper · December 2014

Zhirong Shen
American Bureau of Shipping

De-Cheng Wan
Shanghai Jiao Tong University

RANS SIMULATIONS OF FREE MANEUVERS WITH MOVING RUDDERS AND PROPELLERS USING OVERSET GRIDS IN OPENFOAM

Zhirong Shen (NAOCE and SKLOE-Shanghai Jiao Tong University, China)
Decheng Wan (NAOCE and SKLOE-Shanghai Jiao Tong University, China)
Pablo M. Carrica (IIHR-The University of Iowa, USA)

SUMMARY

This paper presents RANS simulations of free maneuvers with rotating propeller and moving rudders. A dynamic overset grid technique is implemented into the open source code OpenFOAM. The propellers and rudders move with respect to the appended ship, which in turn responds to 6DOF equations of motion. Use of an inertial coordinate systems makes possible to perform full CFD simulations of free maneuvers. SUGGAR is used to generate the domain connectivity information (DCI) to exchange information between overset grids. The free maneuver simulations were performed for three ship models (DTMB 5415M, KVLCC2 and KCS), comprising one zigzag and one turning circle for each geometry.

1. INTRODUCTION

CFD simulations of free maneuvers are challenging due to the complexity of the problem, especially regarding dynamic mesh capabilities. The motions of hull, rudders and propellers are fully coupled during the simulations, requiring full ship 6DOF motions with free surface flow and rotations of the rudder and propeller with respect to the ship hull. Conventional dynamic grid techniques, such as deforming and sliding grids methods, are difficult and inefficient to handle the motions of the ship, rudder and propeller simultaneously. The overset grid technique is an effective solution to the problems described above. Overset grids bypass restrictions of mesh topology in different objects and allow grids to move independently within the computational domain. Computations such as self-propulsion and free maneuvers with discretized propellers and rudders in calm water or waves, very hard to perform with traditional approaches, can be easily handled with overset grids.

Only a limited number of CFD computations of free maneuvers with direct simulation of moving appendages are available in the literature, and most were carried out using overset grids. Carrica et al. [1] discretized the rudders of fully appended DTMB 5415M by overset grid method and performed the zigzag and turn maneuvers with a body force model for the twin propellers in calm water and waves. Mofidi and Carrica [2] applied the same approach for two zigzag maneuvers of KCS. Both propeller and rudder were modelled using the overset grid technique, and excellent results compared with experiments were obtained.

In this paper, zigzag and turn maneuvers using dynamic overset grids with the open source code, OpenFOAM [3] are presented. The CFD solver naoeFoam-os[6,7,10], which adds dynamic overset capabilities to OpenFOAM, is used in this paper to perform the simulations. The ship models DTMB 5415M, KVLCC2 and KCS are the test geometries. One zigzag and one turning circle maneuvers are performed for each ship model. All computational results have been submitted to SIMMAN 2014 for the blind tests in the workshop.

2. OVERSET GRIDS

A dynamic overset grid technique has been implemented into OpenFOAM, which enables a hierarchy of objects and allows the ship hull (parent) to have full 6DOF motions in a free surface flow and rudder and propeller (children) to move independently with respect to the ship hull. The domain connectivity information (DCI) used to build the connection among overset grids is generated using SUGGAR [4]. The flow field is solved by OpenFOAM. OpenFOAM and SUGGAR run simultaneously in different processors and exchange data at the end of each time step. The exchange of data between them is based on MPI and optimized using simultaneous execution of SUGGAR groups in multiple lagged mode, the same method applied in CFDShip-Iowa [5]. SUGGAR runs in serial mode but the communication between OpenFOAM and SUGGAR processors is fully parallel. The DCI from SUGGAR is decomposed based on the domain decomposition of OpenFOAM and each sub-block is sent to a specific processor. For details of the implementation of dynamic overset in OpenFOAM the reader is referred to references [6,7,10].

3. NUMERICAL METHODS

OpenFOAM-2.0 [8] is used to solve the flow field. The computational domain is discretized using the finite volume method (FVM) with arbitrary general polyhedrons. The incompressible Reynolds Averaged Navier-Stokes (RANS) equations are solved iteratively with the PISO algorithm. Volume of Fluid (VOF) with artificial compression technique is used to capture the two-phase air/water interface. The $k-\omega$ SST model [9] is chosen for turbulence closure.

4. CONDITIONS AND RESUTLS

DTMB 5415M, KVLCC2 and KCS are chosen for the computations of free maneuvers. For each ship model, one zigzag and one turning circle maneuvers are carried out. In all cases, rudders and propellers are fully discretized with overset grids and allowed to move and rotate with respect to the ship hull to provide thrust force and turning moment for the ship. All ship models have full 6DOF motions during the simulations.

4.1. DTMB 5415M

The first ship model is DTMB 5415M, built by MARIN. The scale factor of this model is 35.480 and the ship length is 4.002 m. DTMB 5415M is a fully appended surface combatant, with twin propellers and rudders installed. It is also appended with one pair of stabilizer fins, two pairs of bilge keels, shafts and struts, and skeg. The overset grids for DTMB 5415M are shown in Fig. 1. There are six overset component grids for the computations, one for the background, one for the ship hull, two for the twin rudders and the other two for the propellers. Local refinements are added at the free-surface, in the wake and downstream of the propellers. The grids are generated with SnappyHexMesh in OpenFOAM with arbitrary polyhedral cells. Details of the overset system for DTMB 5415M are listed in Table 1.

The approach ship speed is 2.59 m/s, corresponding to *Fr*=0.413. Before the free maneuvers are carried out, a self-propulsion run is performed to determine the propeller speed, resulting in 189.9 RPM in full scale. The propeller RPM is then fixed and used for the maneuvers.

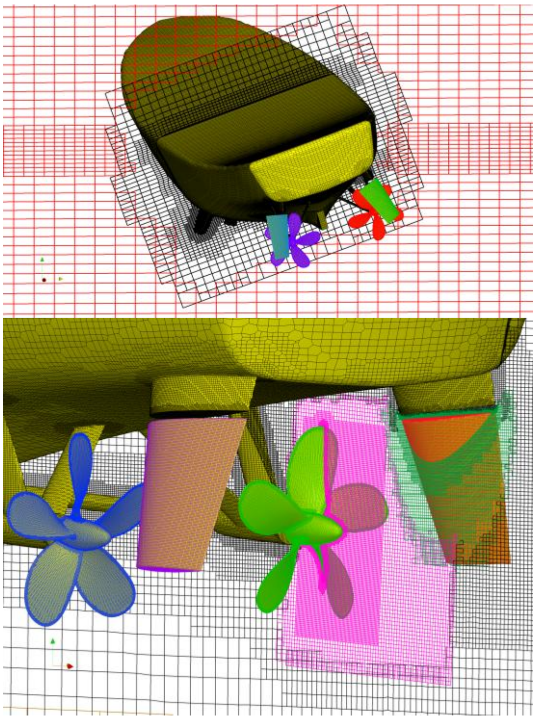

Fig. 1 Overset grids for DTMB 5415M

Table 1 Details of the overset grids for DTMB5415M

Grid Name	Cell number
Background	1,294,596
Hull	2,439,393
Propeller (Port)	1,492,188
Propeller (Starboard)	1,492,188
Rudder (Port)	339,591
Rudder (Starboard)	339,591
Total	7,397,547

The first case is a 20/20 zigzag maneuver. The rudders are first executed to starboard, and two and half zigzag periods are computed. Fig. 2 shows the time evolution of the yaw and rudder angles and yaw rate. The ship model achieves periodic motion after one zigzag period. The overshoot is 4.5^{o} for the first period and reaches 4.8^{o} at the second period. Fig. 3 shows the time histories of drift and roll angles during the zigzag maneuver. The drift angle shows the similar trends as the yaw rate and changes periodically within $\pm 6.8^{o}$. The roll angle peaks at 6^{o} every time the rudders end an execute.

The second case is a turning circle maneuver with 35^{o} rudder deflection. The rudders are deflected to port, with a pull-out executed at 360^{o} heading. Fig. 4 shows the trajectory of the turning circle maneuver. The figure presents a circular trajectory for the steady turn followed by a straight line after the pull-out. Fig. 5 illustrates the roll angle and yaw rate. The rudder execution produces a large roll excursion, but the subsequent oscillation damps out rapidly during the steady turn and pull-out due to the effects of stabilizer fins, bilge keels and skeg.

The time history of yaw rate shows that the ship model reaches a steady turn condition a very short time after rudder execution, indicating a good turning performance.

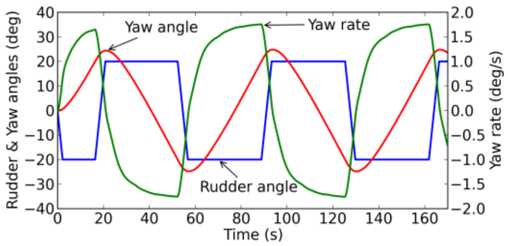

Fig. 2 Time history of rudder and yaw angles and yaw rate for zigzag maneuver for DTMB 5415M

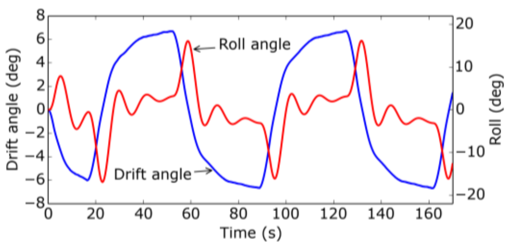

Fig. 3 Time history of drift and roll angles during zigzag maneuver for DTMB 5415M

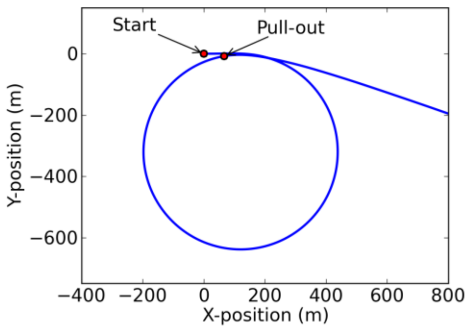

Fig. 4 Trajectory during the turning circle maneuver for DTMB 5415M

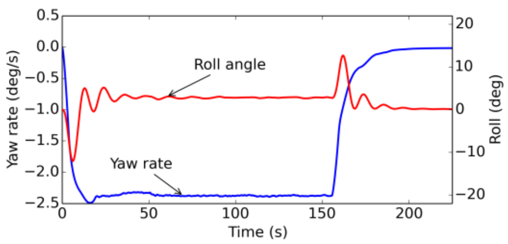

Fig. 5 Time history of drift and roll angles during turning circle maneuver for DTMB 5415M

Fig. 6 presents vortical structures during the turning circle maneuver after the ship has covered half circle and achieves steady state. Vortices detaching from rudders, propellers and other appendages can be clearly observed. The shedding vortices travel from starboard to port side. Fig. 7 shows the free surface at the same instant as in Fig. 6. The free surface shows a strong asymmetry due to the drift velocity and rotating trajectory. The bow waves display higher amplitude in the port side.

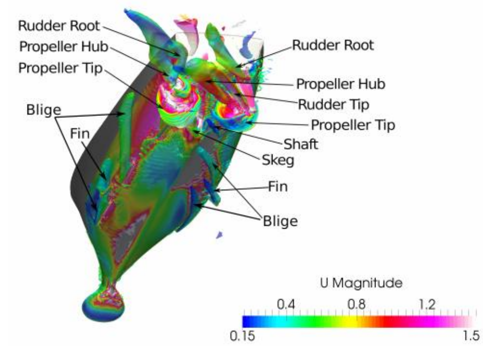

Fig. 6 Vortical structures of DTMB 5415M in the turn maneuver

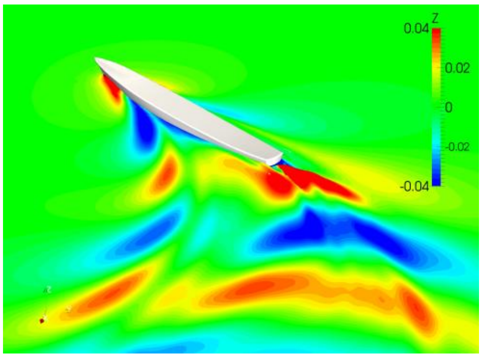

Fig. 7 Free surface colored by elevation for DTMB 5415M in turn maneuver

4.2. KVLCC2

The second ship model is KVLCC2. The model was built by INSEAN. The scale factor is 45.714 and model length is 7.0 m. The approach speed is 1.179 m/s, corresponding to *Fr*=0.142. Maneuvers are performed in deep water. The overset grids are illustrated in Fig. 8. There are four overset component grids, one for the background, one for the hull, one for the rudder and the other for the propeller. The sizes of the grids are listed in Table 2. Once again, all grids are generated with SnappyHexMesh. A self-propulsion run is performed to determine the propeller speed at *Fr*=0.142 before the maneuvers are carried out. The result is 91.96 RPM in full scale.

The first maneuver is a 20/20 zigzag maneuver. The rudder is executed to starboard first. One and half zigzag periods are simulated. Fig. 9 shows the evolution of yaw, yaw rate and rudder angle. The overshoot reaches 13.85° at the first zigzag period and decreases to 10.55° at the second period. The maximum yaw rate is 0.5397 deg/s. KVLLC2 turns much slower than DTMB 5415M due to the slow speed, single rudder and the full form. Fig. 11 shows the time evolution of drift and roll angles. The drift angle changes between -11.4° and 12.9°. The roll angle shows a similar trend as the drift angle. The maximum roll angle is 0.6°, relatively small due to the low speed. In addition, an undamped roll oscillation at the natural can be observed.

The second maneuver is the turning circle maneuver. Restarting from self-propulsion, the rudder is executed to port side at maximum rudder rate to a maximum rudder angle of 35°. The ship model turns 120° and then the pull-out procedure starts. Fig. 11 shows the time history of ship absolute speed and drift angle. The ship speed drops from 15.5 kn and reaches the lowest speed (7.64 kn) after the drift angle reaches the maximum (18.5°). Fig. 12 depicts the evolution of yaw rate and roll angle, which have opposite signs as expected from a center of gravity higher than the waterline. As in the zigzag case, the roll shows undamped oscillations. These oscillations can be caused by poor resolution of the free surface at this low Froude number, and consequent under-estimation of wave radiation. Fig. 13 illustrates the stern vortical structures during the turn maneuver. At this moment, the rudder angle is 35° to the port side. Strong interaction between propeller and rudder can be observed. Two strong vortices from the keel can also be seen.

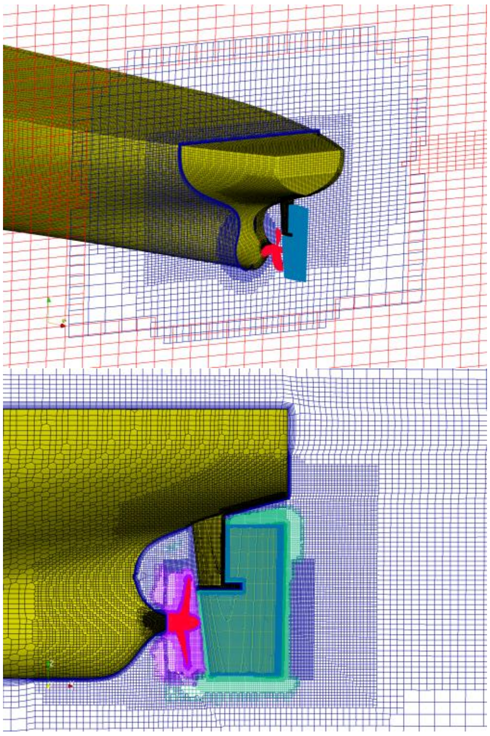
Fig. 8 Overset grids for KVLCC2

Table 2 Details of the overset grids for KVLCC2

Grid Name	Cell Number
Background	821,212
Hull	2,783,667
Propeller	656,078
Rudder	599,235
Total	4,860,192

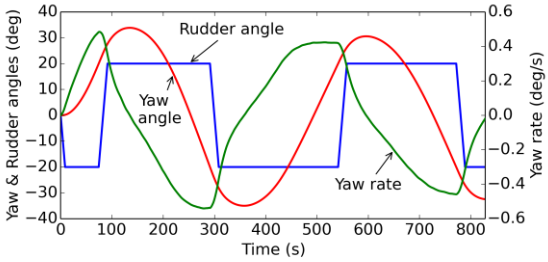

Fig. 9 Time history of the yaw angle, yaw rate and rudder angle during zigzag maneuver for KVLCC2

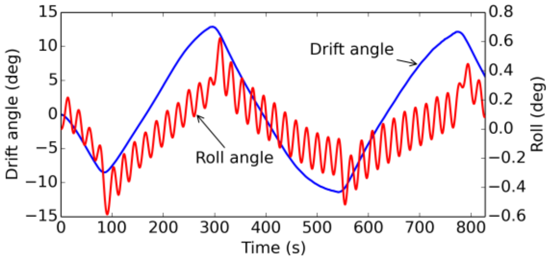

Fig. 10 Time history of the drift and roll angles during zigzag maneuver for KVLCC2

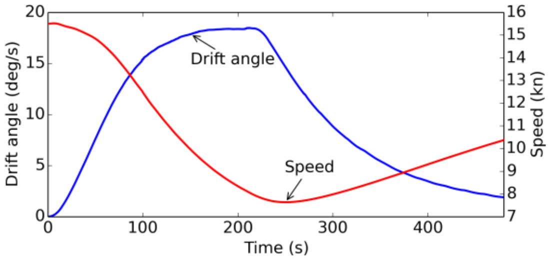

Fig. 11 Time history of the drift angle and ship speed during turn maneuver for KVLCC2

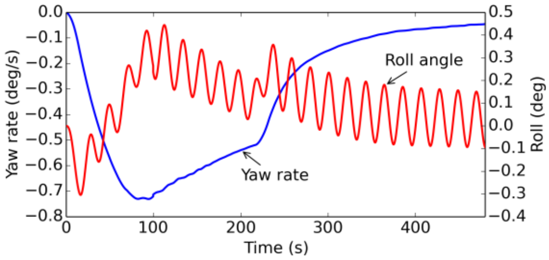

Fig. 12 Time history of the yaw rate and roll angle during turn maneuver for KVLCC2

Table 3 Details of the overset grids for KCS in shallow water

Grid Name	Cell Number
Background	904,972
Hull	2,486,813
Propeller	758,989
Rudder	473,732
Total	4,624,506

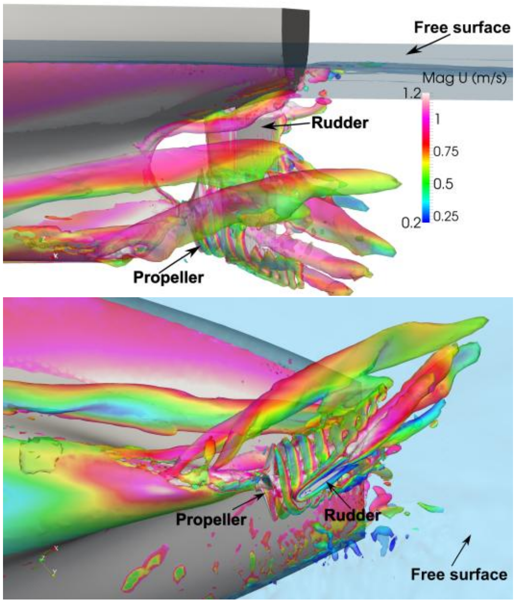

Fig. 13 Vortical structures at the stern of KVLCC2 in the turn maneuver

4.3. KCS in shallow water

The third ship is the SVA KCS model. The scale factor is 52.667 and ship length is 4.3671 m. One zigzag and one turn maneuvers are performed for this model in shallow water. The water depth to draft ratio is h/T=1.2. The approach speed is 0.620 m/s in model scale, corresponding to *Fr*=0.095. The overset grid design is shown in Fig. 14. As for KVLCC2, there are four overset component grids used in the overset assembly for KCS, described in Table 3. In addition to local refinements at the free surface and stern region, the grid between the ship hull and ground bottom is refined to prevent orphans. Again, a self-propulsion computation is carried out to determine the self-propelled propeller rotation speed, which is 46.55 RPM in full scale after the ship speed converges to the target speed. This final self-propelled condition is used as initial condition for the maneuvers.

In the 20/5 zigzag maneuver, the maximum rudder angle is 20^o and the heading change angle is 5^o. The rudder deflects to starboard first. Fig. 15 presents the time history of yaw, yaw rate and rudder angle. Three zigzag periods are performed. The ship reaches periodic behavior after half zigzag period. The maximum overshoot and yaw rate are 3.6^o and 0.227 deg/s, respectively, occurring after one zigzag period. Fig. 16 depicts the evolution of drift and roll angles. The drift angle is closely related to the yaw rate. The roll motion shows a high frequency oscillation, the same phenomenon observed in the case of KVLCC2, but is better damped, likely by a combination of a more boxy shape, relatively larger appendages, and the presence of the solid boundary condition at the bottom. The amplitude of the roll is small, with a maximum at 1.688^o.

For the turn maneuver, the maximum rudder angle is 35^o with the rudder turning to port at maximum rudder rate. Fig. 17 shows the trajectory of the turn maneuver. The ship turns 360^o and then resets the rudder to zero degrees to pull out. Fig. 18 depicts the time evolution of yaw rate and roll angle. Both show strong oscillations at the beginning of the turn maneuver. The yaw rate converges to 0.245 deg/s and the roll angle converges to 0.88^o. Fig. 19 illustrates the vortical systems at the stern, shown as iso-surfaces of Q colored by absolute velocity. The vortices are mainly generated by rudder and propeller. No vortex is seen near the ship keel due to the presence of the solid bottom. The vortices are weaker than those of KVCCL2 and DTMB 5415M.

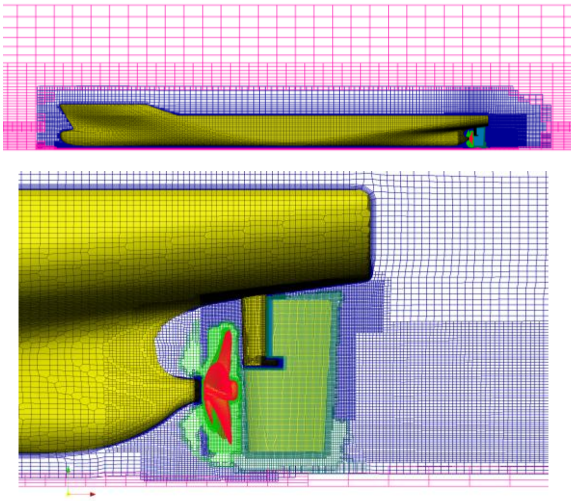

Fig. 14 Overset grids for KCS in shallow water

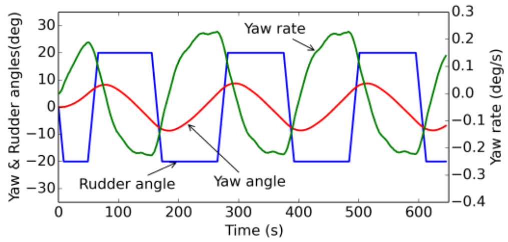

Fig. 15 Time history of yaw angle, yaw rate and rudder angle during the zigzag maneuver for KCS in shallow water

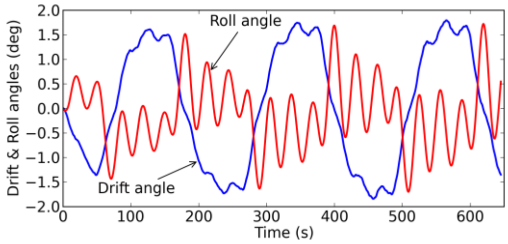

Fig. 16 Time history of drift and roll angles during the zigzag maneuver for KCS in shallow water

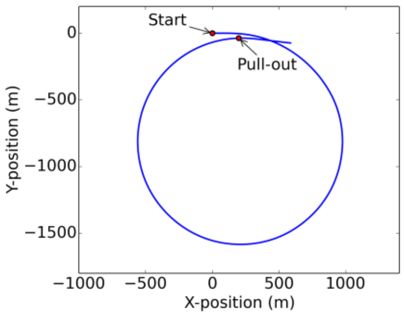

Fig. 17 Trajectory of the turning circle maneuver for KCS in shallow water

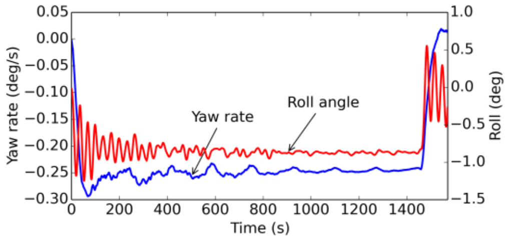

Fig. 18 Time history of the yaw rate and roll angle during the turn maneuver for KCS in shallow water

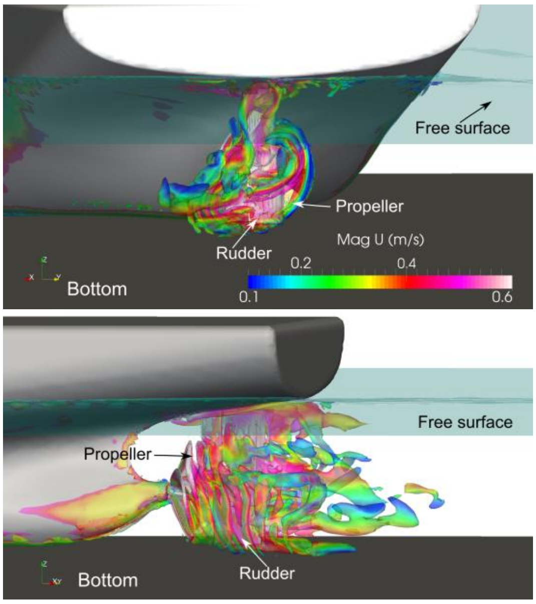

Fig. 19 Vortices at the stern of KCS in shallow water during the turn maneuver

5. CONCLUSIONS

In this paper, RANS simulations zigzag and turn maneuvers are presented. The simulations of DTMB 5415M, KVLCC2 and KCS are performed by the CFD solver naoeFoam-os, in which the dynamic overset grid technique has been successfully implemented in OpenFOAM. The approach shows great flexibility and the ability to perform complex computations with relatively coarse grids.

6. ACKNOWLEDGEMENTS

The authors thank IIHR-Hydroscience and Engineering for hosting Mr. Zhirong Shen's visit to The University of Iowa and provide the research environment for the development of part of the work. The visit of Mr. Zhirong Shen to The University of Iowa was supported by the China Scholarship Council. The support of National Natural Science Foundation of China (Grant Nos. 51379125, 51411130131, 11432009), Program for Professor of Special Appointment at Shanghai Institutions of Higher Learning (Grant No. 2013022), National Key Basic Research Development Plan Project of China (Grant No. 2013CB036103) and Lloyd's Register Foundation, are acknowledged. Computations were performed at the Helium HPC cluster at The University of Iowa.

7. REFERENCES

[1] PM Carrica, F Ismail, M Hyman, S Bhushan, F Stern, "Turn and zigzag maneuvers of a surface combatant using a URANS approach with dynamic overset grids," J. Mar. Sci. Technol., 18, 166–181, 2013.

[2] A Mofidi, PM Carrica, "Simulations of zigzag maneuvers for a container ship with direct moving rudder and propeller," Comput. Fluids, 96, 191–203, 2014.

[3] "Official Website of OpenFOAM." http://www.openfoam.com/.

[4] RW Noack, "SUGGAR: a general capability for moving body overset grid assembly," AIAA 2005-5117, 17th AIAA Comput. Fluid Dyn. Conf., Toronto, Ontario, Canada, 2005.

[5] PM Carrica, J Huang, R Noack, D Kaushik, B Smith, F Stern, "Large-scale computations of the forward speed diffraction and pitch and heave problems for a surface combatant," Comput. Fluids, 39, 1095–1111, 2010.

[6] Z Shen, DC Wan, PM Carrica, "Self-Propulsion Simulation of KCS with Dynamic Overset Grids," 8th Int. OpenFOAM Workshop, Jeju, Korea, 2013.

[7] Z Shen, DC Wan, PM Carrica, "Dynamic Overset Grids in OpenFOAM with Application to KCS Self-Propulsion and Maneuvering," Submitted to Ocean Eng., 2014.

[8] "OpenFOAM User Guide Version-2.0," OpenCFD Ltd., 2011.

[9] FR Menter, M Kuntz, R Langtry, "Ten years of industrial experience with the SST turbulence model," Turb. Heat Mass Trans. 4, 625–632, 2003.

[10] Z Shen, DC Wan, PM Carrica, "Ship Motions of KCS in Head Waves with Rotating Propeller Using Overset Grid Method," Proc. OMAE-2014, San Francisco, USA.